The American Journal of Human Genetics, Volume *105*

Supplemental Data

Exome-Derived Adiponectin-Associated Variants Implicate Obesity and Lipid Biology

Cassandra N. Spracklen, Tugce Karaderi, Hanieh Yaghootkar, Claudia Schurmann, Rebecca S. Fine, Zoltan Kutalik, Michael H. Preuss, Yingchang Lu, Laura B.L. Wittemans, Linda S. Adair, Matthew Allison, Najaf Amin, Paul L. Auer, Traci M. Bartz, Matthias Blüher, Michael Boehnke, Judith B. Borja, Jette Bork-Jensen, Linda Broer, Daniel I. Chasman, Yii-Der Ida Chen, Paraskevi Chirstofidou, Ayse Demirkan, Cornelia M. van Duijn, Mary F. Feitosa, Melissa E. Garcia, Mariaelisa Graff, Harald Grallert, Niels Grarup, Xiuqing Guo, Jeffrey Haesser, Torben Hansen, Tamara B. Harris, Heather M. Highland, Jaeyoung Hong, M. Arfan Ikram, Erik Ingelsson, Rebecca Jackson, Pekka Jousilahti, Mika Kähönen, Jorge R. Kizer, Peter Kovacs, Jennifer Kriebel, Markku Laakso, Leslie A. Lange, Terho Lehtimäki, Jin Li, Ruifang Li-Gao, Lars Lind, Jian'an Luan, Leo-Pekka Lyytikäinen, Stuart MacGregor, David A. Mackey, Anubha Mahajan, Massimo Mangino, Satu Männistö, Mark I. McCarthy, Barbara McKnight, Carolina Medina-Gomez, James B. Meigs, Sophie Molnos, Dennis Mook-Kanamori, Andrew P. Morris, Renee de Mutsert, Mike A. Nalls, Ivana Nedeljkovic, Kari E. North, Craig E. Pennell, Aruna D. Pradhan, Michael A. Province, Olli T. Raitakari, Chelsea K. Raulerson, Alex P. Reiner, Paul M. Ridker, Samuli Ripatti, Neil Roberston, Jerome I. Rotter, Veikko Salomaa, America A. Sandoval-Zárate, Colleen M. Sitlani, Tim D. Spector, Konstantin Strauch, Michael Stumvoll, Kent D. Taylor, Betina Thuesen, Anke Tönjes, Andre G. Uitterlinden, Cristina Venturini, Mark Walker, Carol A. Wang, Shuai Wang, Nicholas J. Wareham, Sara M. Willems, Ko Willems van Dijk, James G. Wilson, Ying Wu, Jie Yao, Kristin L. Young, Claudia Langenberg, Timothy M. Frayling, Tuomas O. Kilpeläinen, Cecilia M. Lindgren, Ruth J.F. Loos, and Karen L. Mohlke

SUPPLEMENTAL FIGURES

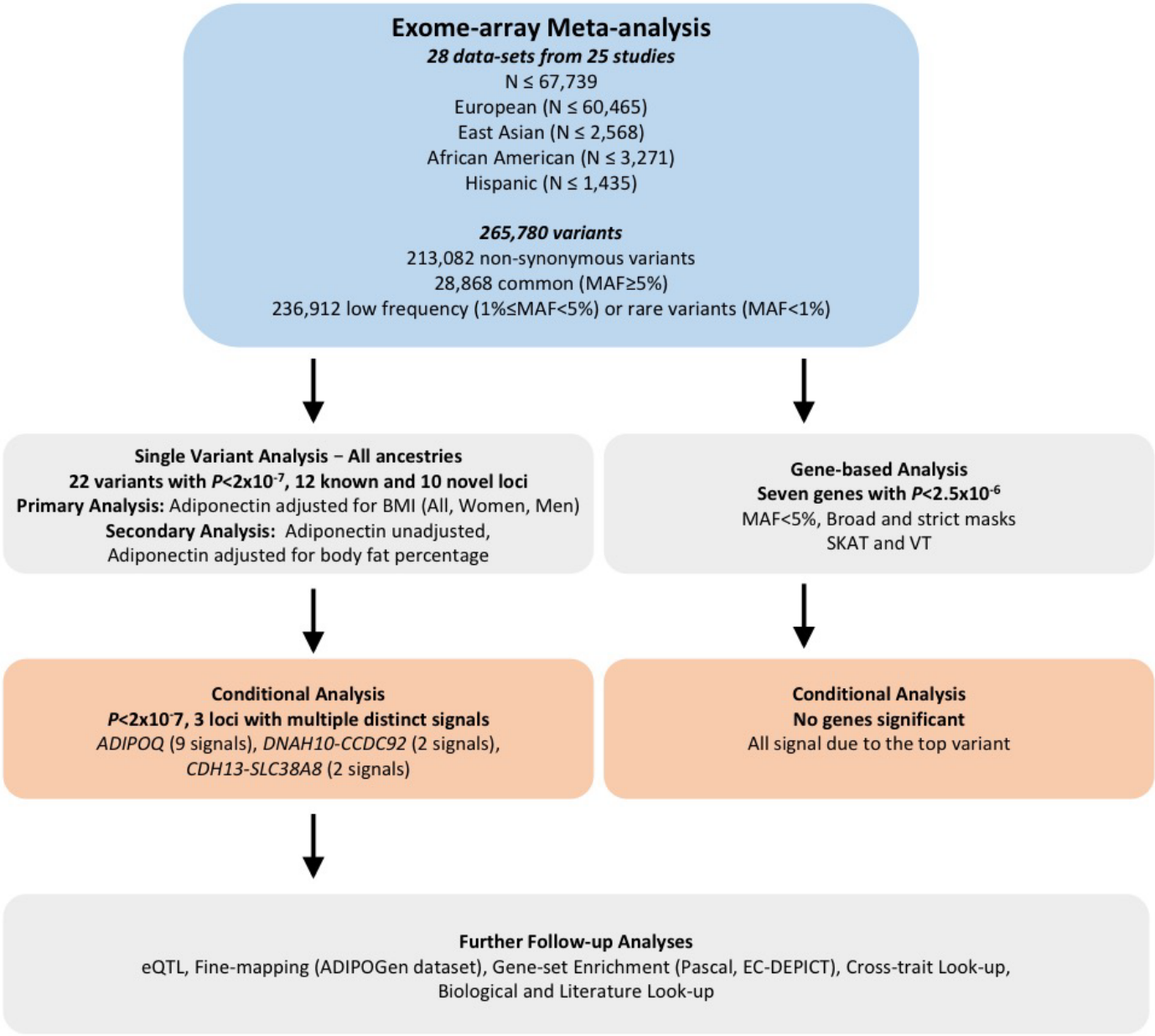

Figure S1. Workflow for the adiponectin exome-array meta-analysis and follow-up analyses.
MAF, minor allele frequency; BMI, body mass index.

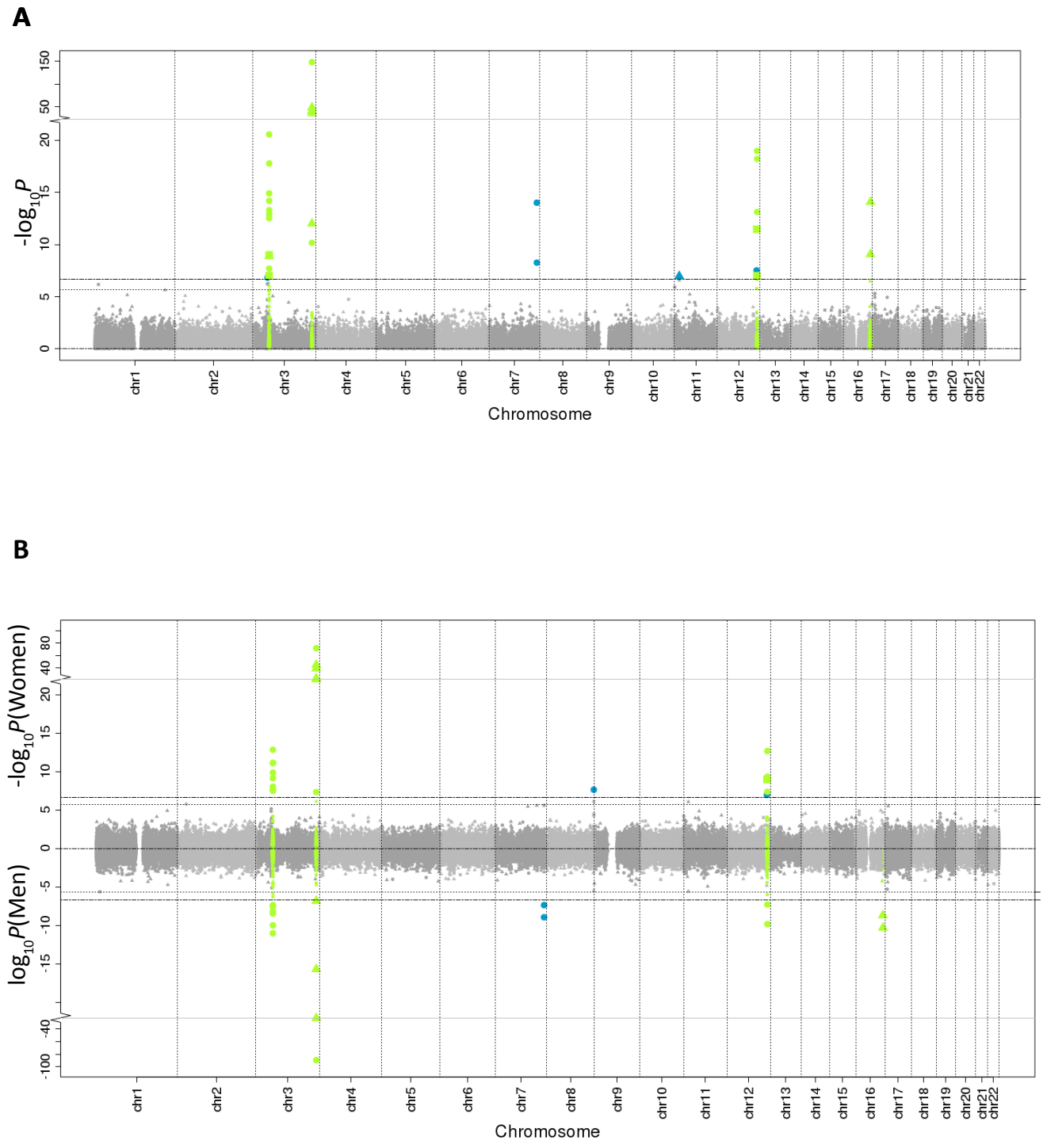

Figure S2. Adiponectin association results for models unadjusted for BMI or fat percentage. (A) Manhattan plot showing the exome-wide variants in the adiponectin unadjusted analysis [X-axis: Chromosome number; Y-axis: $-\log_{10}(P)$ for the all ancestries sex-combined additive model]. Green highlighted variants show the previously identified loci that also achieved $P<2\times10^{-6}$ in this dataset. Horizontal lines mark *P*-value thresholds 2×10^{-7} (top; array-wide significance level) and 2×10^{-6} (suggestive; bottom). (B) Miami plot showing the exome-wide variants in sex-specific analyses [X-axis: Chromosome number; Top panel y-axis: $-\log_{10}P$(Women); Bottom panel y-axis: $-\log_{10}P$(Men) for the all ancestries additive model]. Green highlighted variants show the previously identified loci that also achieved $P<2\times10^{-6}$ in each dataset. Horizontal lines mark *P*-value thresholds 2×10^{-7} (array-wide significance level) and 2×10^{-6} (suggestive). Circles, triangles, squares correspond to MAF≥0.05, MAF<0.01 and MAF<0.05, respectively. Blue symbols represent novel associations achieving $P<2\times10^{-7}$.

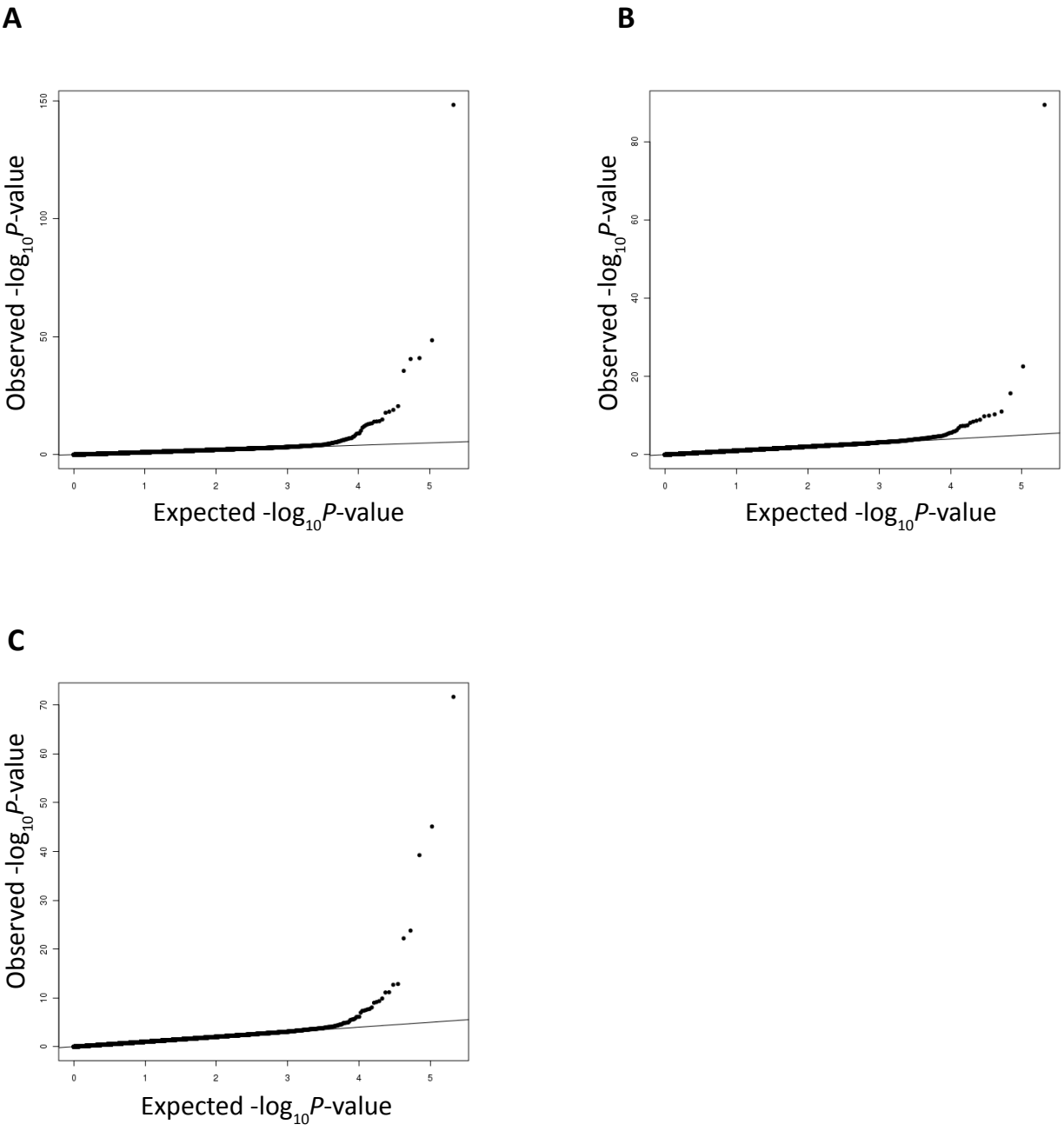

Figure S3. QQ plots of the exome-wide variants in the adiponectin unadjusted analysis
[X-axis: Expected $-\log_{10}(P)$; Y-axis: Observed $-\log_{10}(P)$]. (A) All ancestries sex-combined additive model; (B) All ancestries men-specific additive model; (C) All ancestries women-specific additive model.

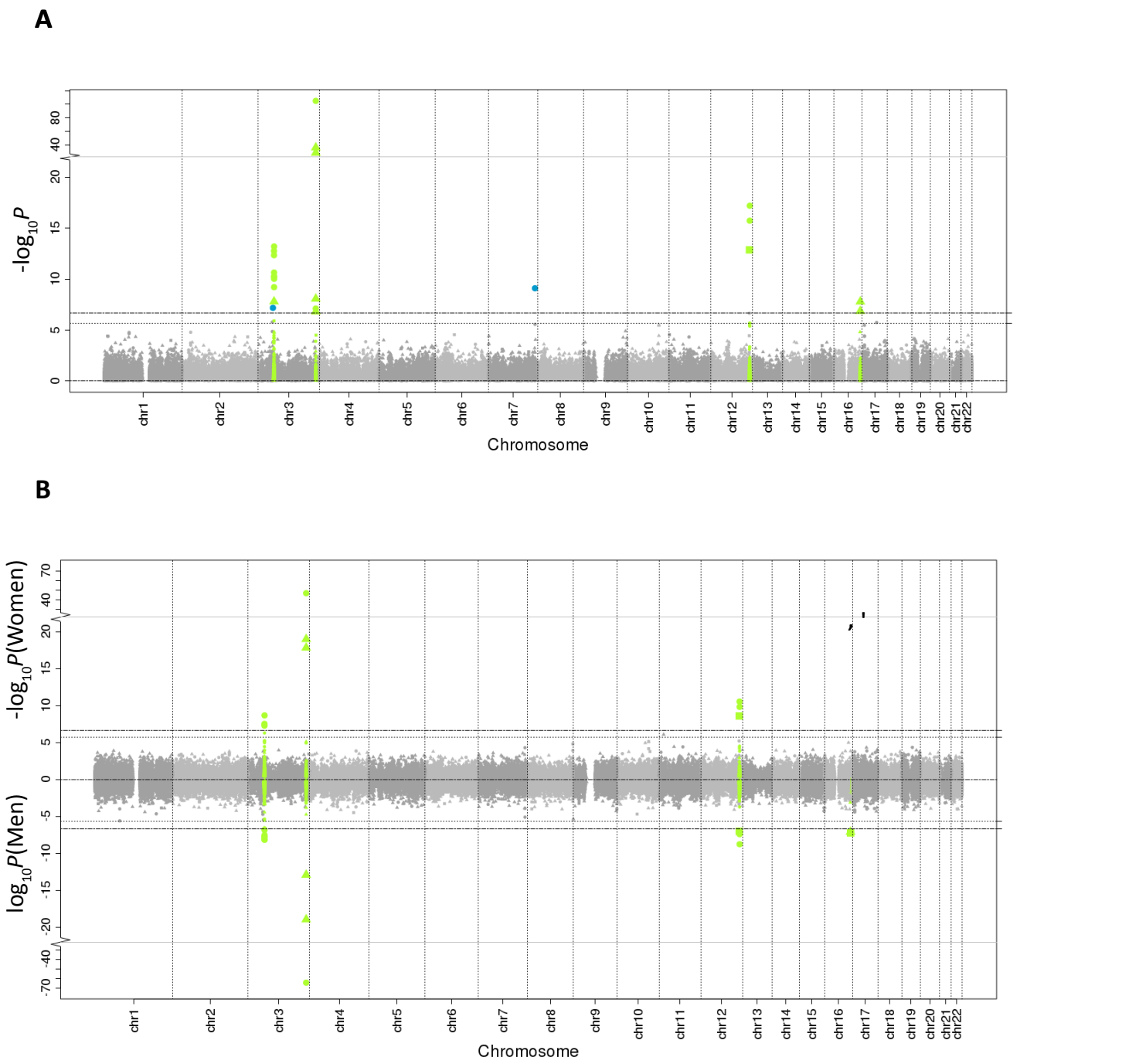

Figure S4. Adiponectin associaiton results for models adjusted for fat percentage.
(A) Manhattan plot showing the exome-wide variants in the adiponectin adjusted for fat percentage analysis [X-axis: Chromosome number; Y-axis: $-\log_{10}(P)$ for the all ancestries sex-combined additive model]. Green highlighted variants show the previously identified loci that also achieved $P<2\times10^{-6}$ in this dataset. Horizontal lines mark *P*-value thresholds 2×10^{-7} (top; array-wide significance level) and 2×10^{-6} (suggestive; bottom). (B) Miami plot showing the exome-wide variants in sex-specific analyses [X-axis: Chromosome number; Top panel y-axis: $-\log_{10}P$(Women); Bottom panel y-axis: $-\log_{10}P$(Men) for the all ancestries additive model]. Green highlighted variants show the previously identified loci that also achieved $P<2\times10^{-6}$ in each dataset. Horizontal lines mark *P*-value thresholds 2×10^{-7} (array-wide significance level) and 2×10^{-6} (suggestive). Circles, triangles, squares correspond to MAF≥0.05, MAF<0.01 and MAF<0.05, respectively. Blue symbols represent novel associations with $P<2\times10^{-7}$.

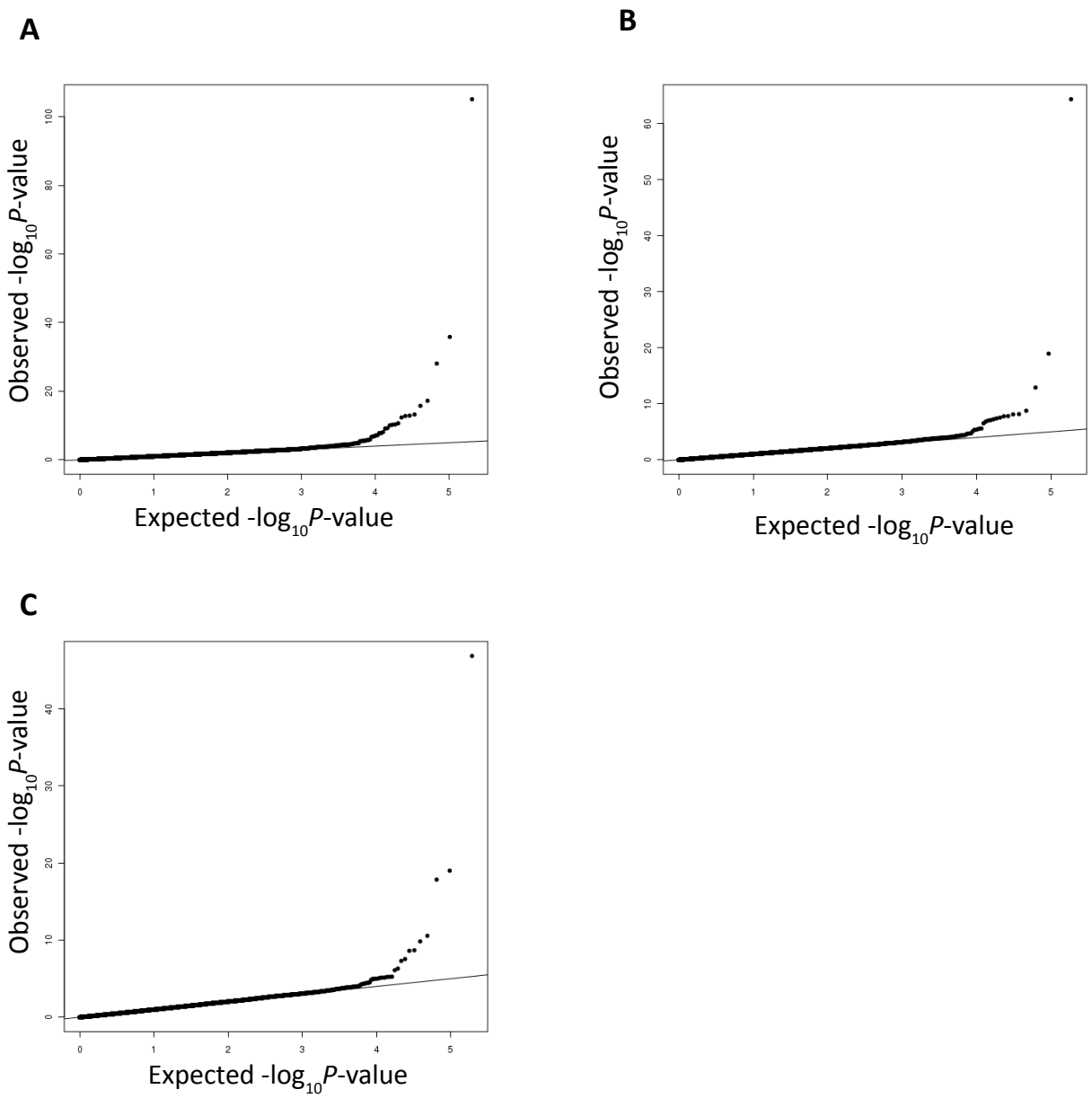

Figure S5. QQ plots showing the exome-wide variants in the adiponectin adjusted for fat percent analysis [X-axis: Expected –$\log_{10}$(P); Y-axis: Observed -$\log_{10}$(P)]. (A) All ancestries sex-combined additive model; (B) All ancestries men-specific additive model; (C) All ancestries women-specific additive model.

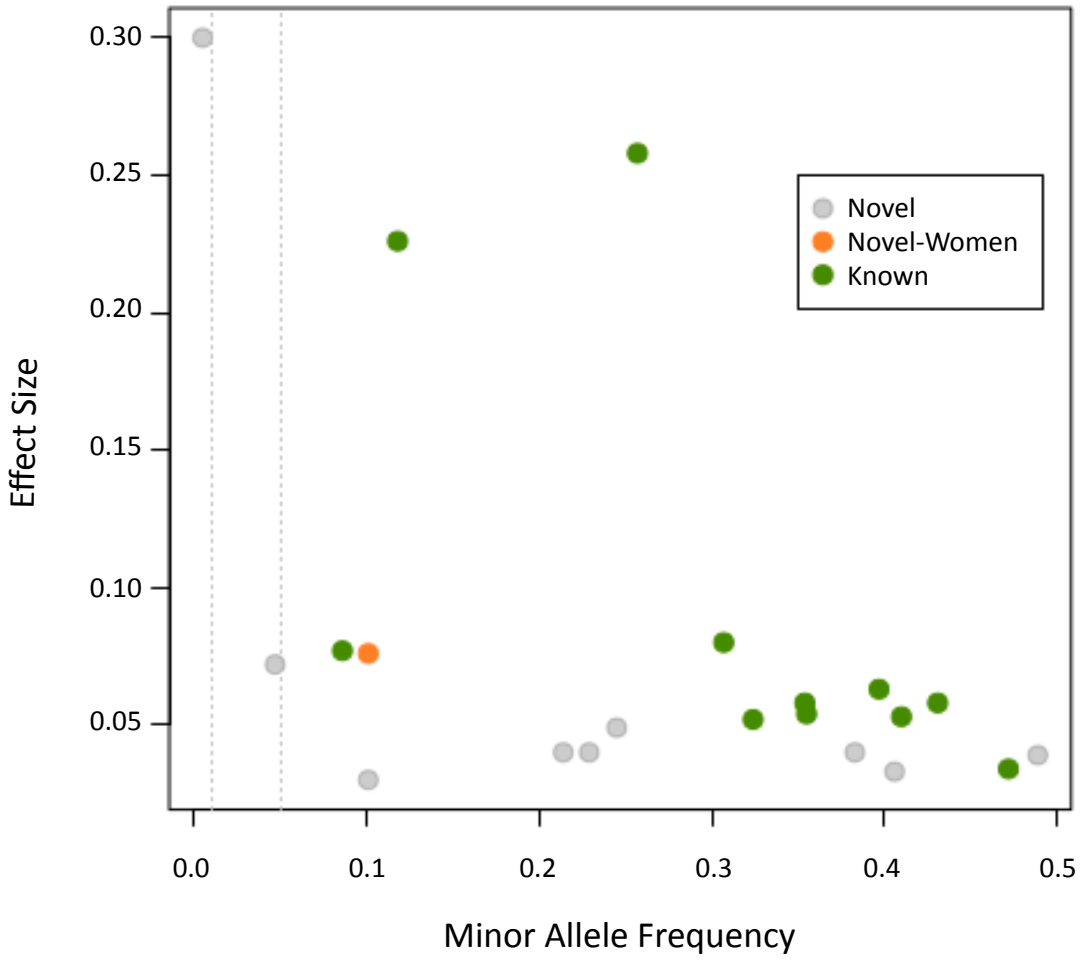

Figure S6. Effect size vs. minor allele frequency (MAF) for variants in the primary adiponectin analysis [X-axis: MAF; Y-axis: effect size for the all ancestries, sex-combined and women-specific additive model]. Gray, orange, and green variants show the novel and previously identified loci that also achieved $P<2x10^{-7}$ in the combined and women-specific analyses as labeled. Vertical lines mark MAF=0.01 and MAF=0.05.

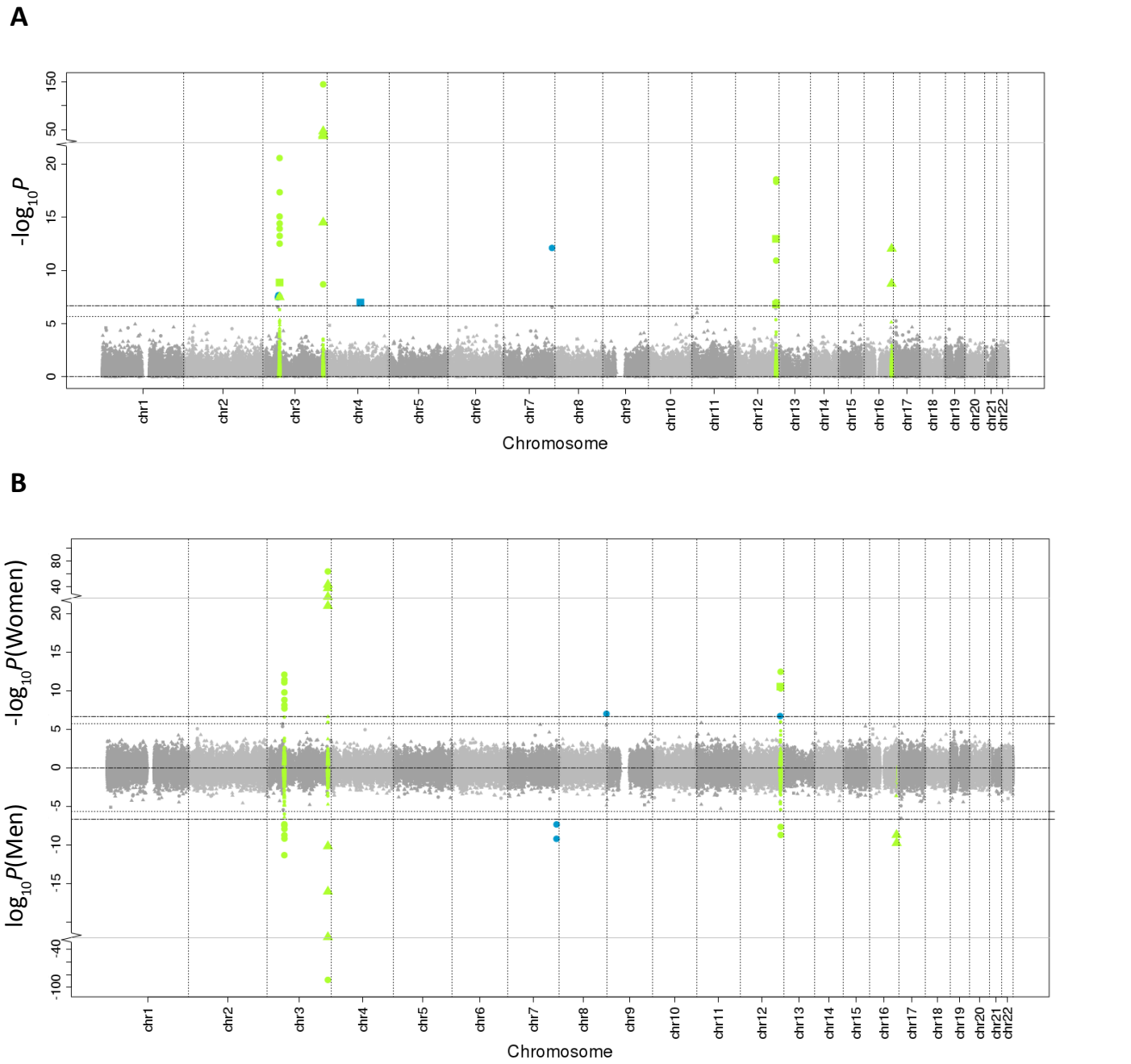

Figure S7. Adiponectin associaiton results for models adjusted for BMI.
(A) Manhattan plot showing the exome-wide variants in the adiponectin adjusted for body mass index analysis [X-axis: Chromosome number; Y-axis: $-\log_{10}(P)$ for the all ancestries sex-combined additive model]. Green highlighted variants show the previously identified loci that also achieved $P<2\times10^{-6}$ in this dataset. Horizontal lines mark *P*-value thresholds 2×10^{-7} (top; array-wide significance level) and 2×10^{-6} (suggestive; bottom). (B) Miami plot showing the exome-wide variants in sex-specific analyses [X-axis: Chromosome number; Top panel y-axis: $-\log_{10}(P_{WOMEN})$; Bottom panel y-axis: $-\log_{10}(P_{MEN})$ for the all ancestries additive model]. Green highlighted variants show the previously identified loci that also achieved $P<2\times10^{-6}$ in each dataset. Horizontal lines mark *P*-value thresholds 2×10^{-7} (array-wide significance level) and 2×10^{-6} (suggestive). Circles, triangles, squares correspond to MAF≥0.05, MAF<0.01 and MAF<0.05, respectively. Blue symbols represent novel associations wtih $P<2\times10^{-7}$.

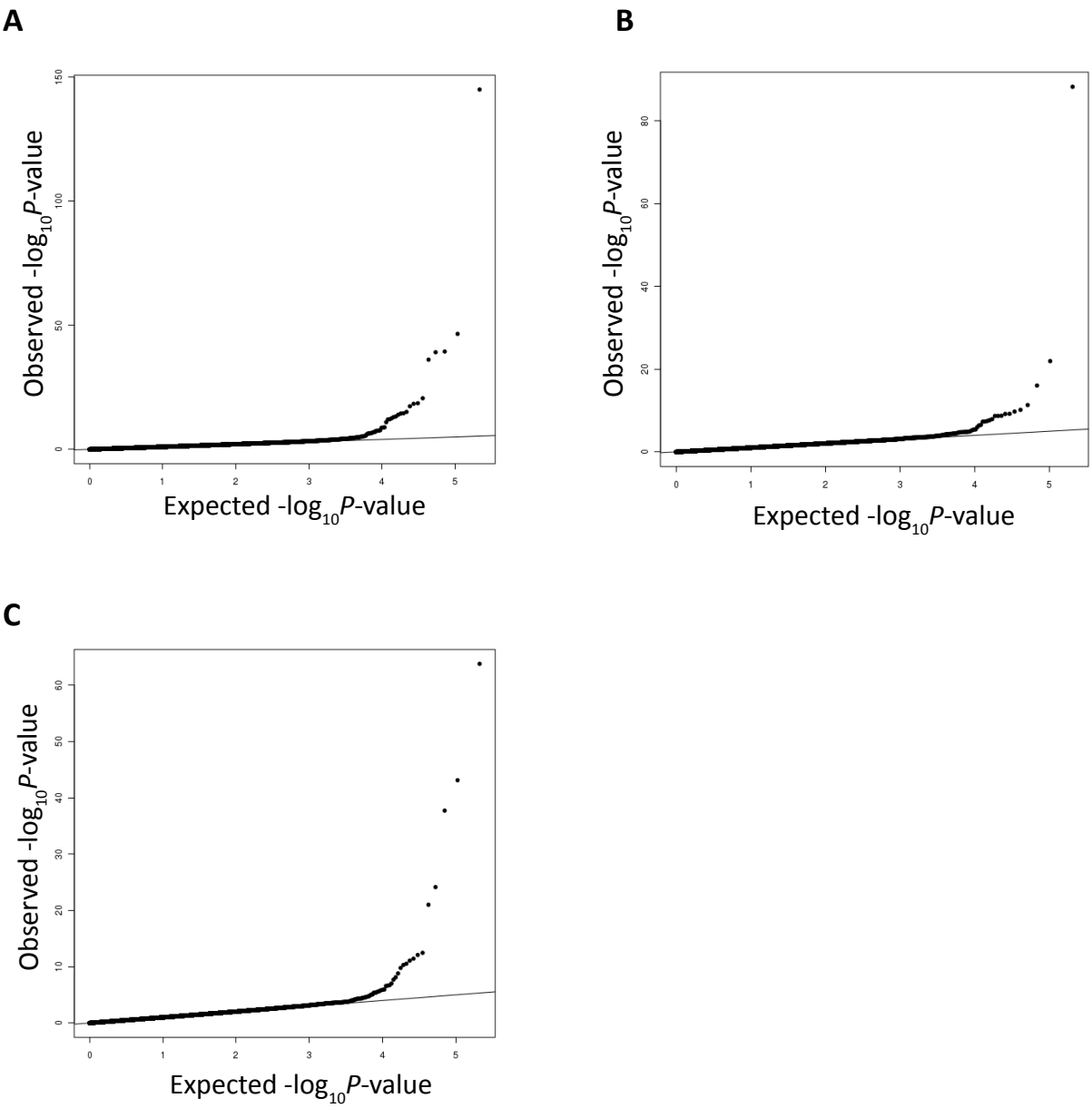

Figure S8. QQ plots showing the exome-wide variants in the adiponectin adjusted for BMI analysis [X-axis: Expected –log10(P); Y-axis: Observed -log10(P)]. (A) All ancestries sex-combined additive model; (B) All ancestries men-specific additive model; (C) All ancestries women-specific additive model.

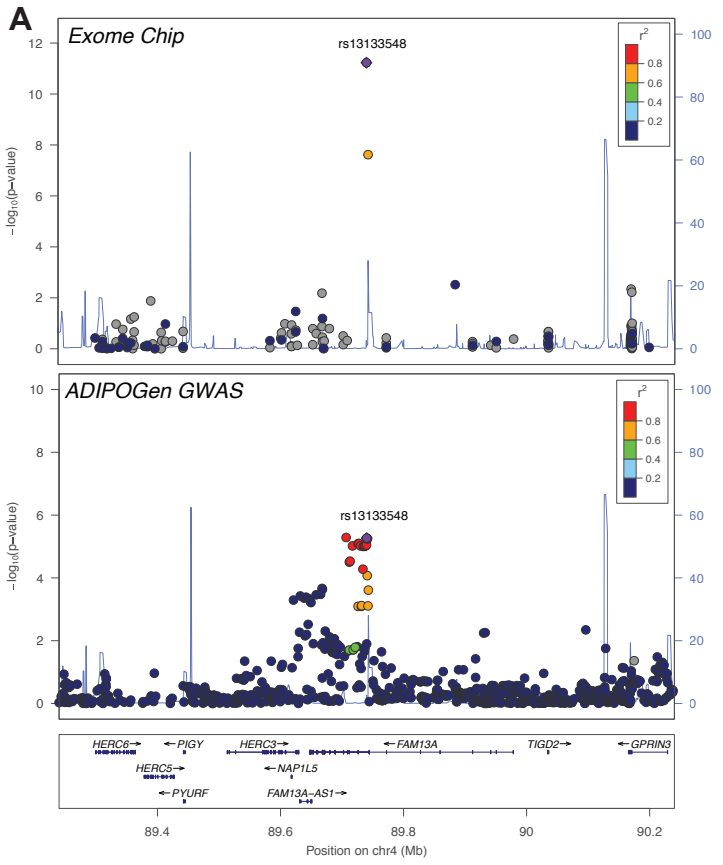
A
Exome Chip
rs13133548
ADIPOGen GWAS
rs13133548
HERC6
PIGY
HERC3
FAM13A
TIGD2
GPRIN3
HERC5
NAP1L5
PYURF
FAM13A-AS1
89.4
89.6
89.8
90
90.2
Position on chr4 (Mb)
−log10(p-value)
Recombination rate (cM/Mb)

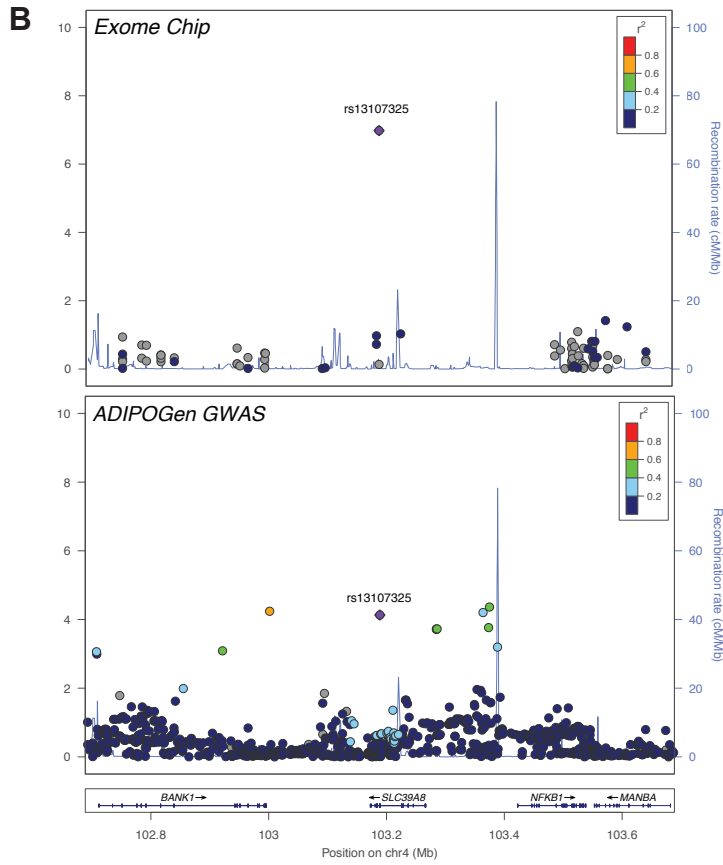
B
Exome Chip
rs13107325
ADIPOGen GWAS
rs13107325
BANK1
SLC39A8
NFKB1
MANBA
102.8
103
103.2
103.4
103.6
Position on chr4 (Mb)
Recombination rate (cM/Mb)

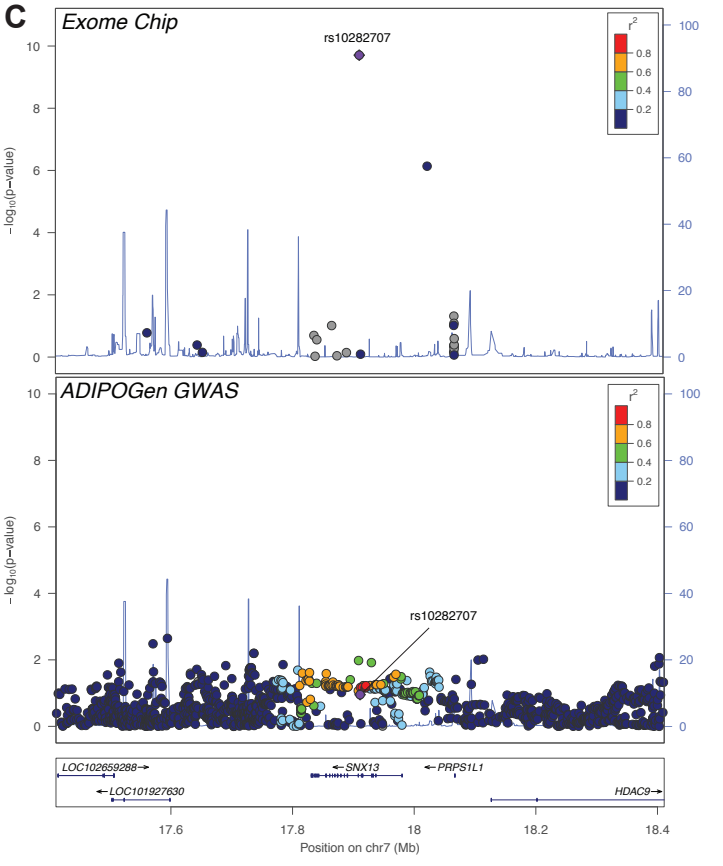
C
Exome Chip
rs10282707
ADIPOGen GWAS
rs10282707
LOC102659288
SNX13
PRPS1L1
LOC101927630
HDAC9
17.6
17.8
18
18.2
18.4
Position on chr7 (Mb)
−log10(p-value)

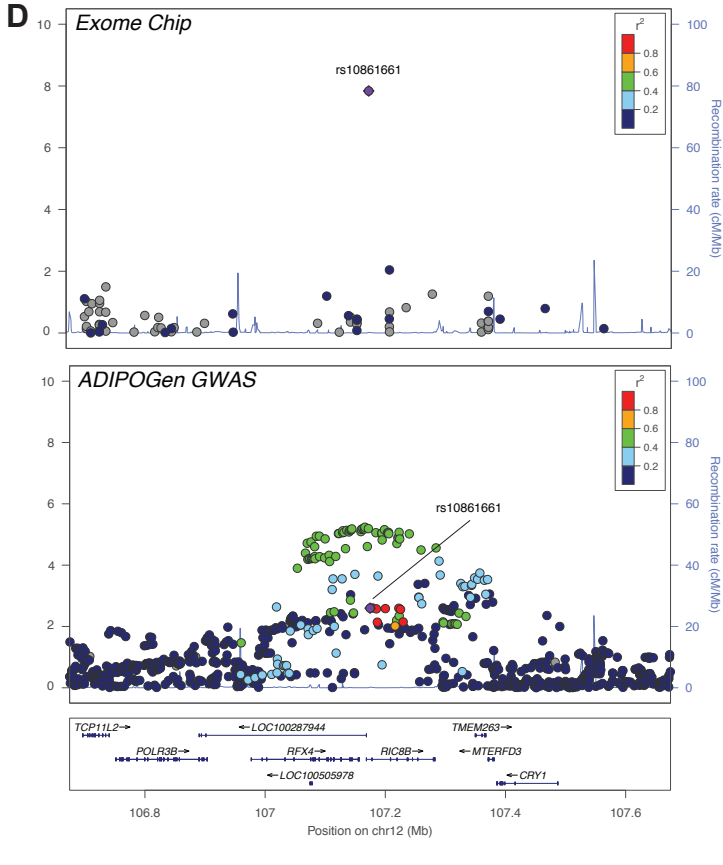
D
Exome Chip
rs10861661
ADIPOGen GWAS
rs10861661
TCP11L2
LOC100287944
TMEM263
POLR3B
RFX4
RIC8B
MTERFD3
LOC100505978
CRY1
106.8
107
107.2
107.4
107.6
Position on chr12 (Mb)
Recombination rate (cM/Mb)

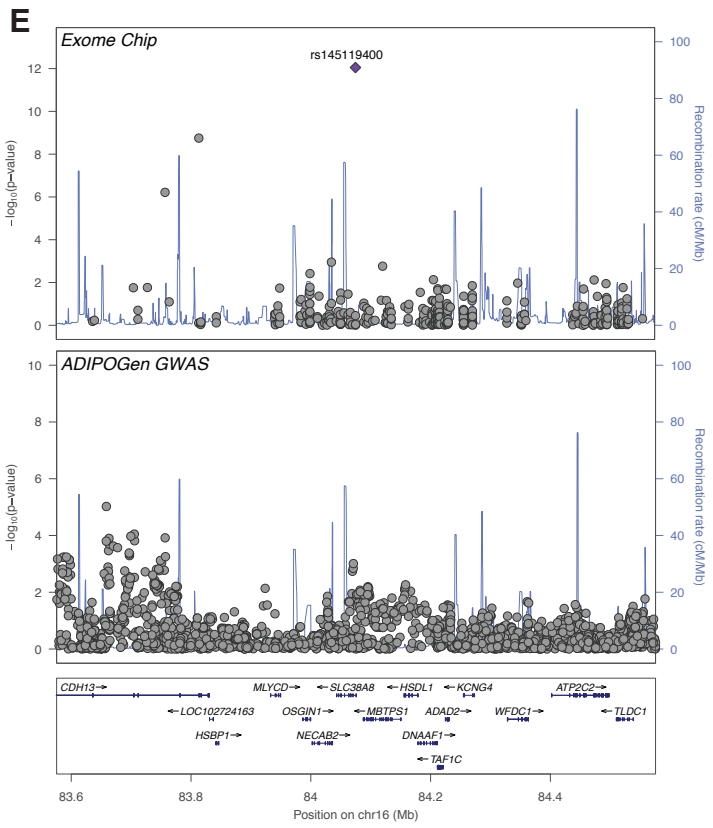

Figure S9. Plots of five previously unreported adiponectin-associated loci in sex-combined exome-wide meta-analysis.

A) *FAM13A*, B) *SLC39A8*, C) *SNX13*, D) *RIC8B*, and E) *SLC38A8*. The upper plots show the current exome-wide meta-analysis, and the lower plots show the genome-wide ADIPOGen consortium meta-analysis from Dastani, et al., 2012. In E, rs145119400 was not included in the ADIPOGen consortium meta-analysis. Each point represents a variant in the meta-analysis, plotted with P-value (on a -log10 scale) on the y-axis and genomic position (hg19) on the x-axis. In each plot, the index variant identified in the exome chip meta-analysis is represented in purple, and the color of all other variants indicate the LD with the index variant in European ancestry haplotypes from the 1000 Genome Phase 3 reference panel. In A, C, and D, the lead variant from the exome-wide analysis may not be the best representative of the adiponectin-associated signal.

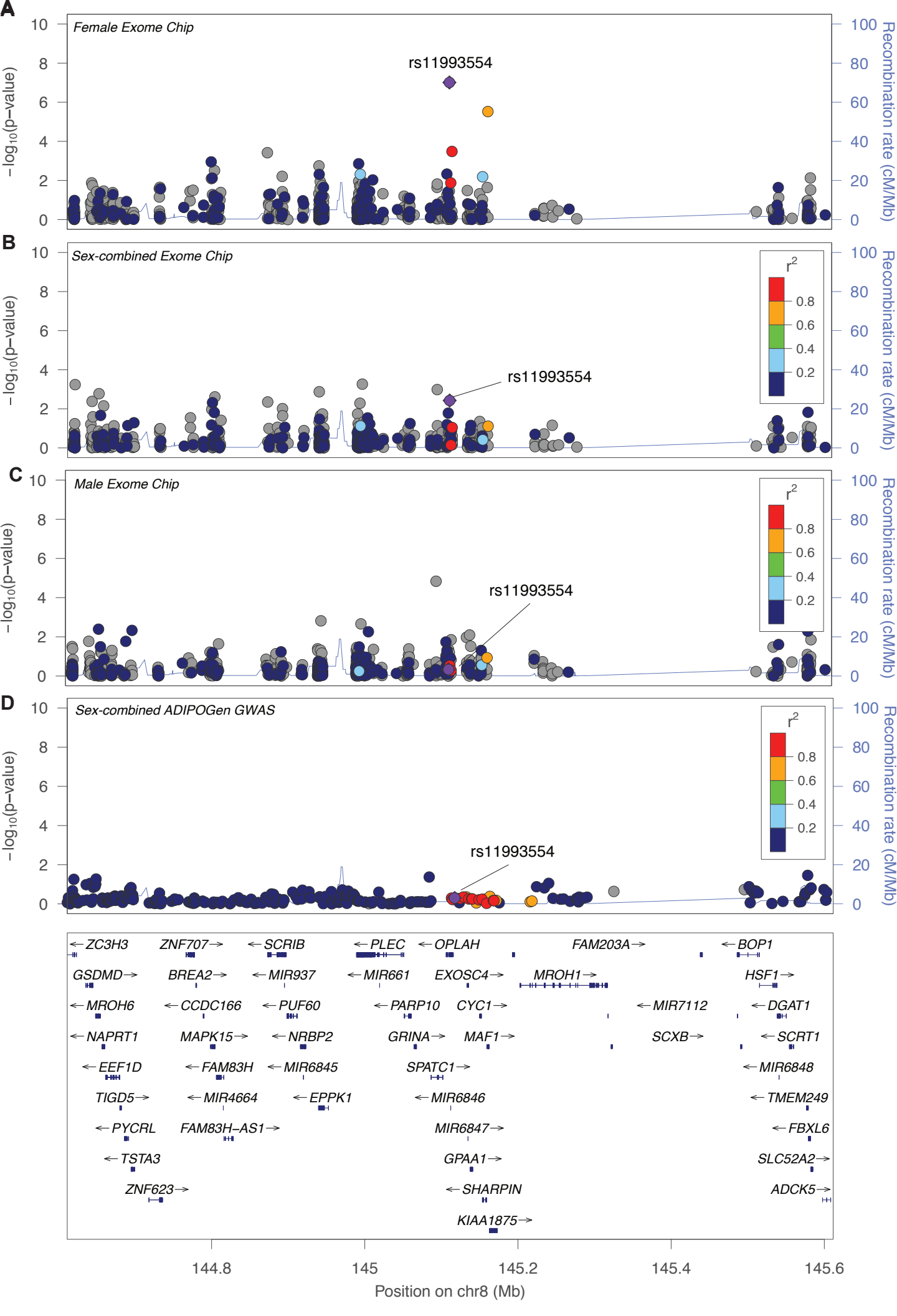
A
Female Exome Chip
rs11993554
B
Sex-combined Exome Chip
rs11993554
C
Male Exome Chip
rs11993554
D
Sex-combined ADIPOGen GWAS
rs11993554
−log10(p−value)
Recombination rate (cM/Mb)
r2
0.8
0.6
0.4
0.2
ZC3H3
ZNF707
SCRIB
PLEC
OPLAH
FAM203A
BOP1
GSDMD
BREA2
MIR937
MIR661
EXOSC4
MROH1
HSF1
MROH6
CCDC166
PUF60
PARP10
CYC1
MIR7112
DGAT1
NAPRT1
MAPK15
NRBP2
GRINA
MAF1
SCXB
SCRT1
EEF1D
FAM83H
MIR6845
SPATC1
MIR6848
TIGD5
MIR4664
EPPK1
MIR6846
TMEM249
PYCRL
FAM83H−AS1
MIR6847
FBXL6
TSTA3
GPAA1
SLC52A2
ZNF623
SHARPIN
ADCK5
KIAA1875
144.8
145
145.2
145.4
145.6
Position on chr8 (Mb)

Figure S10. **Plot of novel adiponectin-associated OPLAH only observed in females**. A) Females only from exome-wide meta-analysis, B) Sex-combined results from exome-wide meta-analysis, C) Males only from exome-wide meta-analysis, and D) Sex-combined genome-wide ADIPOGen meta-analysis. Each point represents a variant in the meta-analysis, plotted with P-value (on a -log10 scale) on the y-axis and genomic position (hg19) on the x-axis. In each plot, the index variant identified in the exome chip meta-analysis is represented in purple, and the color of all other variants indicate the LD with the index variant in European ancestry haplotypes from the 1000 Genome Phase 3 reference panel. Sex-specific data were not available from the ADIPOGen consortium meta-analysis.

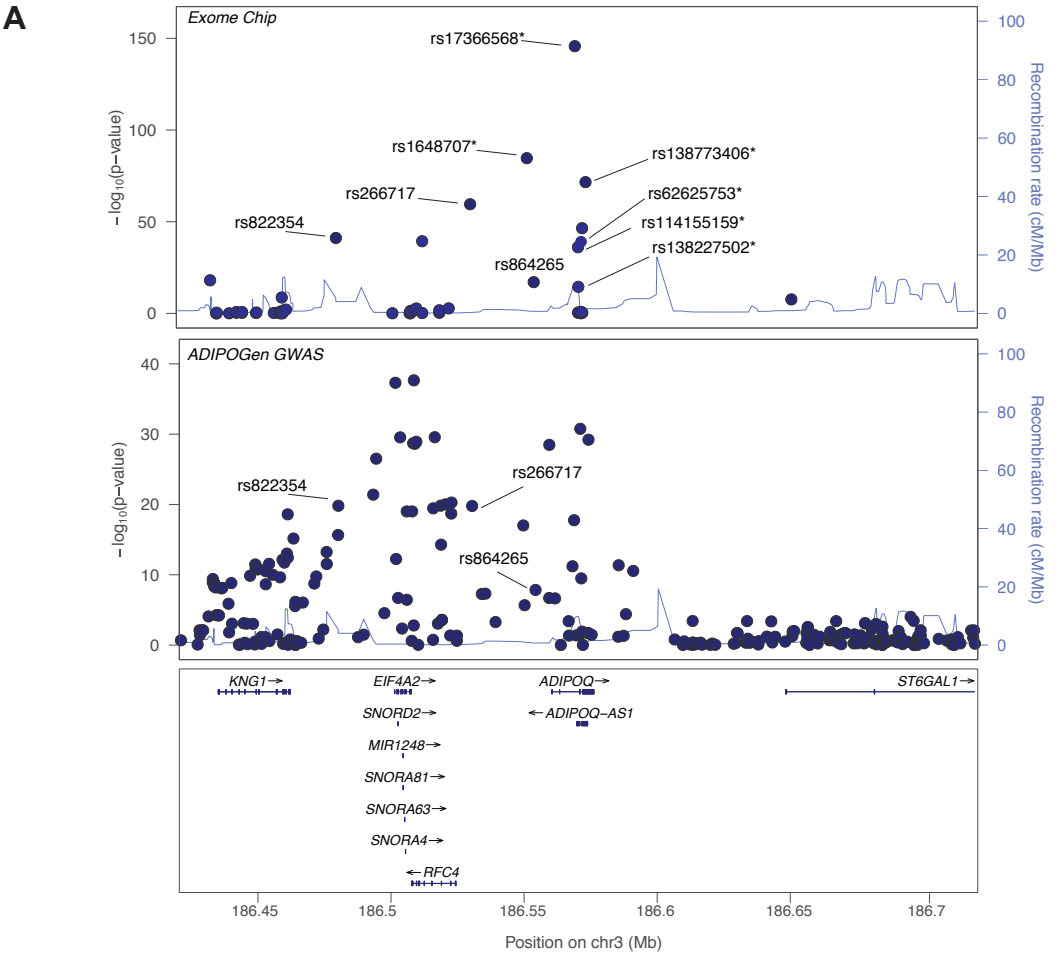
A
Exome Chip
rs17366568*
rs1648707*
rs138773406*
rs266717
rs62625753*
rs822354
rs114155159*
rs138227502*
rs864265
ADIPOGen GWAS
rs822354
rs266717
rs864265
KNG1
EIF4A2
ADIPOQ
ST6GAL1
SNORD2
ADIPOQ-AS1
MIR1248
SNORA81
SNORA63
SNORA4
RFC4
186.45
186.5
186.55
186.6
186.65
186.7
Position on chr3 (Mb)
– log10(p–value)
Recombination rate (cM/Mb)

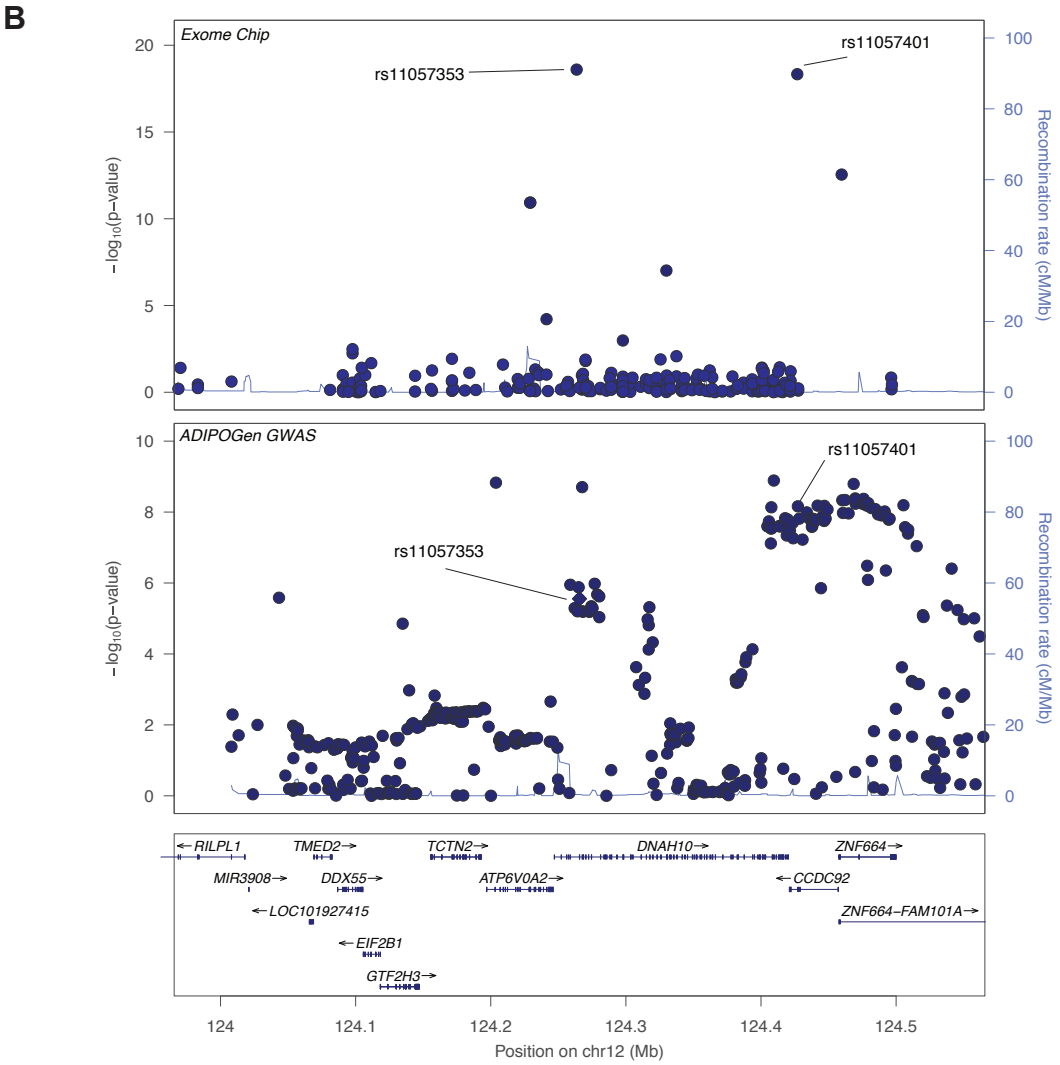
B
Exome Chip
rs11057401
rs11057353
ADIPOGen GWAS
rs11057401
rs11057353
RILPL1
TMED2
TCTN2
DNAH10
ZNF664
MIR3908
DDX55
ATP6V0A2
CCDC92
LOC101927415
ZNF664–FAM101A
EIF2B1
GTF2H3
124
124.1
124.2
124.3
124.4
124.5
Position on chr12 (Mb)
– log10(p–value)
Recombination rate (cM/Mb)

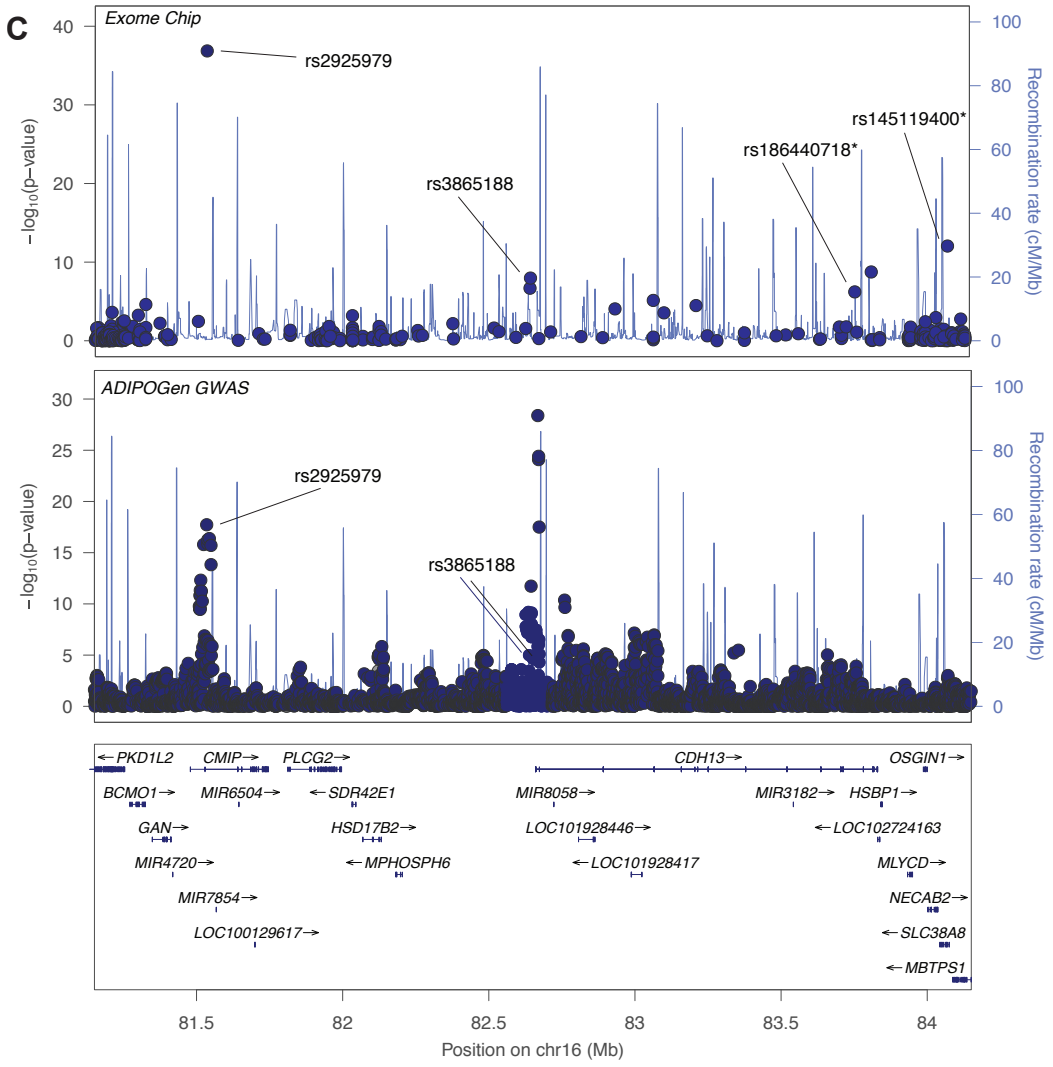

Figure S11. **Three adiponectin loci exhibit multiple distinct association signals.** A) ADIPOQ with nine exome-wide association signals, B) DNAH10-CCDC92 with two exome-wide association signals, and C) CDH13-region with four exome-wide association signals. Each point represents a variant in the meta-analysis, plotted with P-value (on a -log10 scale) on the y-axis and genomic position (hg19) on the x-axis. Asterisks (*) indicate variants identified as a distinct association signal in the Exome Chip analysis but were not present in the ADIPOGen data. Given that many noncoding variants were not tested in this exome-wide analysis, the number of signals and lead variants may differ in genome-wide analyses..

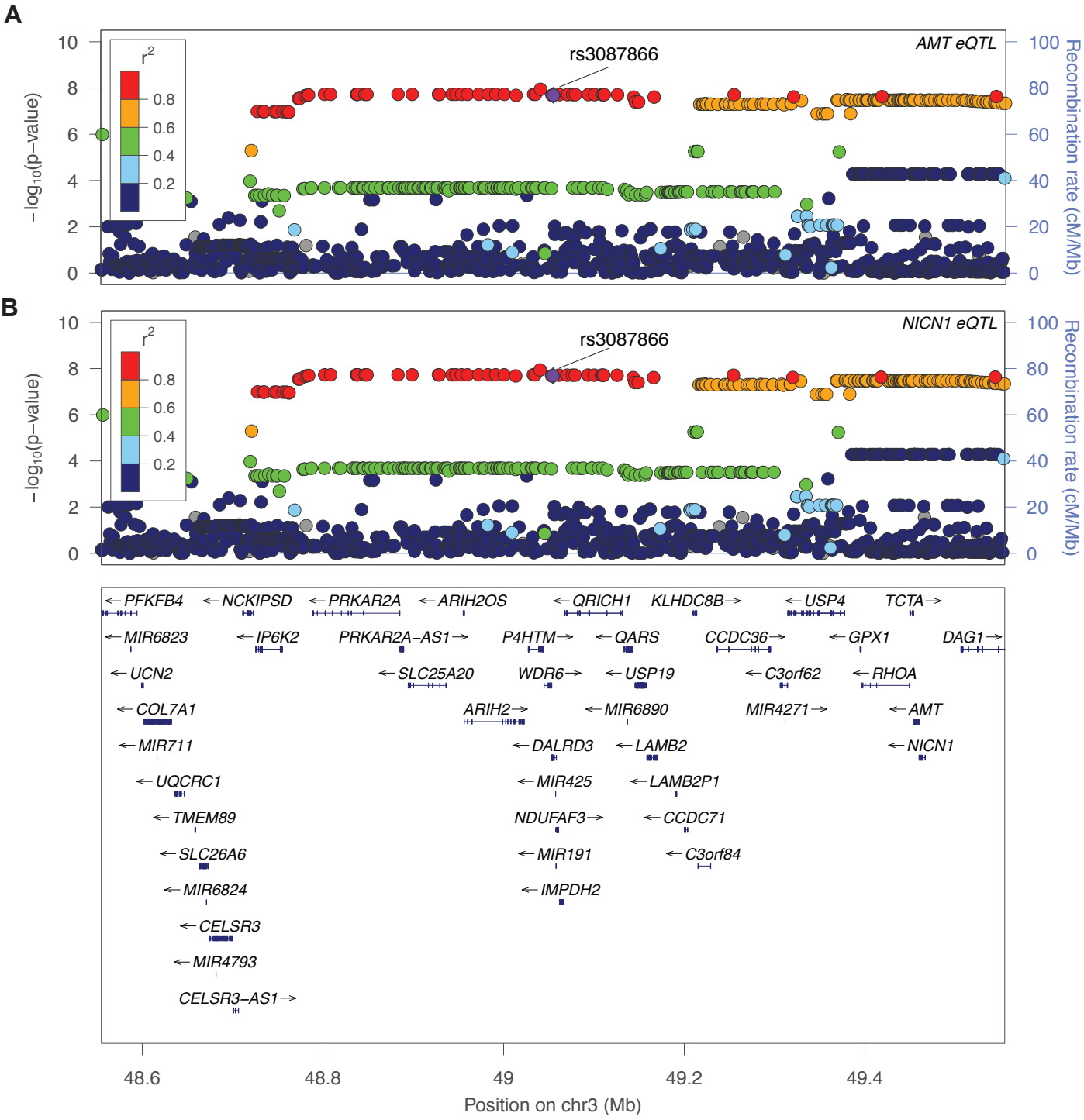

Figure S12. Subcutaneous adipose eQTLs for AMT and NICN1 colocalize with the DALRD3 novel adiponectin exome-wide locus. rs3087866 (purple diamond) shows the strongest association with adiponectin levels in the exome-wide meta-analysis at this locus). rs3087866 and 85 proxy variants (r^2>0.80; 1000Gp3) are nominally associated with adiponectin levels. The same variants exhibit the strongest association with expression of *AMT* (A) and *NICN1* (B) in subcutaneous adipose tissue. Each point represents a variant in the meta- or eQTL analysis, plotted with their P-value (on a -log10 scale) on the y-axis and genomic position (hg19) on the x-axis. The color of all other variants indicates the LD with the index variant in European ancestry haplotypes from the 1000 Genome Phase 3 reference panel. Based on eQTL colocalization with the adiponectin-associated variants, *AMT*, *NICN1*, and *PRKAR2A* are candidate genes at this locus.

Cohort Funding Information

The **Atherosclerosis Risk in Communities (ARIC)** study is carried out as a collaborative study supported by the National Heart, Lung, and Blood Institute (NHLBI) contracts (HHSN268201100005C, HHSN268201100006C, HHSN268201100007C, HHSN268201100008C, HHSN268201100009C, HHSN268201100010C, HHSN268201100011C, and HHSN268201100012C). The authors thank the staff and participants of the ARIC study for their important contributions. Funding support for "Building on GWAS for NHLBI-diseases: the U.S. CHARGE consortium" was provided by the NIH through the American Recovery and Reinvestment Act of 2009 (ARRA) (5RC2HL102419).

This **CHS** research was supported by NHLBI contracts HHSN268201200036C, HHSN268200800007C, HHSN268201800001C, N01HC55222, N01HC85079, N01HC85080, N01HC85081, N01HC85082, N01HC85083, N01HC85086; and NHLBI grants R01HL068986, U01HL080295, R01HL087652, R01HL105756, R01HL103612, R01HL120393, and U01HL130114 with additional contribution from the National Institute of Neurological Disorders and Stroke (NINDS). Additional support was provided through R01AG023629 from the National Institute on Aging (NIA). A full list of principal CHS investigators and institutions can be found at CHS-NHLBI.org. The provision of genotyping data was supported in part by the National Center for Advancing Translational Sciences, CTSI grant UL1TR000124, and the National Institute of Diabetes and Digestive and Kidney Disease Diabetes Research Center (DRC) grant DK063491 to the Southern California Diabetes Endocrinology Research Center. The content is solely the responsibility of the authors and does not necessarily represent the official views of the National Institutes of Health. Additional grant received from the AHA Clinically Applied Research Grant, R01 HL094555 from NHLBI.

CLHNS thanks the Office of Population Studies Foundation research and data collection teams and the study participants who generously provided their time for this study. This work was supported by National Institutes of Health grants DK078150, TW005596 and HL085144; pilot funds from RR020649, ES010126, and DK056350; and the Office of Population Studies Foundation.

The **Erasmus Rucphen Family** (**ERF)** study is grateful to all study participants and their relatives, general practitioners and neurologists for their contributions and to P. Veraart for her help in genealogy, J. Vergeer for the supervision of the laboratory work and P. Snijders for his help in data collection. ERF was supported by the Consortium for Systems Biology (NCSB), both within the framework of the Netherlands Genomics Initiative (NGI)/Netherlands Organisation for Scientific Research (NWO). ERF study as a part of EUROSPAN (European Special Populations Research Network) was supported by European Commission FP6 STRP grant number 018947 (LSHG-CT-2006-01947) and also received funding from the European Community's Seventh Framework Programme (FP7/2007-2013)/grant agreement HEALTH-F4-2007-201413 by the European Commission under the programme "Quality of Life and Management of the Living Resources" of 5th Framework Programme (no. QLG2-CT-2002-01254) as well as FP7 project EUROHEADPAIN (nr 602633). The ERF study was further supported by ENGAGE consortium and CMSB. High-throughput analysis of the ERF data was supported by joint grant from Netherlands Organization for Scientific Research and the Russian Foundation for Basic Research (NWO-RFBR 047.017.043)The exome-chip measurements have been funded by the Netherlands Organization for Scientific Research (NWO; project number 184021007) and by the Rainbow Project (RP10; Netherlands Exome Chip Project) of the Biobanking and Biomolecular Research Infrastructure Netherlands (BBMRI-NL; www.bbmri.nl (http://www.bbmri.nl)). Ayse Demirkan is supported by a Veni grant (2015) from ZonMw. Ayse Demirkan, Jun Liu and Cornelia van Duijn have used exchange grants from PRECEDI. The funders had no role in study design, data collection and analysis, decision to publish, or preparation of the manuscripts.

The **Fenland Study** is funded by the Wellcome Trust and the Medical Research Council (MC_U106179471). We are grateful to all the volunteers for their time and help, and to the General Practitioners and practice staff for assistance with recruitment. We thank the Fenland Study Investigators, Fenland Study Co-ordination team and the Epidemiology Field, Data and Laboratory teams. We further acknowledge support from the Medical research council (MC_UU_12015/1).

The **FINRISK07/DILGOM** is funded by the Academy of Finland (#118065 and #136895).

The **Framingham Heart Study** (FHS) was initiated in 1948 and is comprised of 5,209 participants from Framingham, MA (US), who have undergone examinations every other year to evaluate cardiovascular disease and related risk factors. The Offspring cohort was recruited in 1971 and includes 5,124 children of the Original cohort and the children's spouses[5]. Participants from the Offspring cohort have attended exams roughly every four years. Adiponectin levels were measured using specimens collected at the 7th exam from the Offspring cohort. The current analysis includes 2,223 individuals with available phenotypic and genotypic information.

The **Inter99** was initiated by Torben Jørgensen (PI), Knut Borch-Johnsen (co-PI), Hans Ibsen and Troels F. Thomsen. The steering committee comprises the former two and Charlotta Pisinger. The study was financially supported by research grants from the Danish Research Council, the Danish Centre for Health Technology Assessment, Novo Nordisk Inc., Research Foundation of Copenhagen County, Ministry of Internal Affairs and Health, the Danish Heart Foundation, the Danish Pharmaceutical Association, the Augustinus Foundation, the Ib Henriksen Foundation, the Becket Foundation, and the Danish Diabetes Association.

We thank the **Jackson Heart Study (JHS**) participants and staff for their contributions to this work. The JHS is supported by contracts HHSN268201300046C, HHSN268201300047C, HHSN268201300048C, HHSN268201300049C, HHSN268201300050C from the National Heart, Lung, and Blood Institute and the National Institute on Minority Health and Health Disparities.

The **KORA** research platform (KORA, Cooperative Research in the Region of Augsburg) was initiated and financed by the Helmholtz Zentrum München – German Research Center for Environmental Health, Neuherberg, Germany and supported by grants from the German Federal Ministry of Education and Research (BMBF), the Federal Ministry of Health (Berlin, Germany), the Ministry of Innovation, Science, Research and Technology of the state North Rhine-Westphalia (Düsseldorf, Germany), and the Munich Center of Health Sciences (MC Health) as part of LMUinnovativ. This research was supported by the European Union's Seventh Framework Programme (FP7-Health-F5-2012) under grant agreement no. 305280 (MIMOmics), by the Helmholtz-Russia Joint Research Group (HRJRG) 310, and by the German Center for Diabetes Research (DZD). We thank all members of field staffs who were involved in the planning and conduct of the MONICA/KORA Augsburg studies. The funders had no role in study design, data collection and analysis, decision to publish, or preparation of the manuscript.

Leipzig-Adults was supported by the Kompetenznetz Adipositas (Competence network for Obesity) funded by the Federal Ministry of Education and Research (German Obesity Biomaterial Bank; FKZ 01GI1128), and by grants from the Collaborative Research Center funded by the German Research Foundation (CRC 1052 "Obesity mechanisms"; B01, B03). IFB Adiposity Diseases is supported by the Federal Ministry of Education and Research (BMBF), Germany, FKZ: 01EO1501 (projects AD2-060E, AD2-06E95, AD2-06E99 to P.K.).

MESA was supported by the Multi-Ethnic Study of Atherosclerosis (MESA) contracts HHSN268201500003I, N01-HC-95159, N01-HC-95160, N01-HC-95161, N01-HC-95162, N01-HC-95163, N01-HC-95164, N01-HC-95165, N01-HC-95166, N01-HC-95167, N01-HC-95168, N01-HC-95169, UL1-TR-000040, UL1-TR-001079, and UL1-TR-001420. The provision of genotyping data was supported in part by the National Center for Advancing Translational Sciences, CTSI grant UL1TR001881, and the National Institute of Diabetes and Digestive and Kidney Disease Diabetes Research (DRC) grant DK063491.

METSIM was supported by Academy of Finland grants 77299, 124243, and 141226; the Finnish Heart Foundation; the Finnish Diabetes Foundation; the Juselius Foundation; the Commission of the European Community HEALTH-F2-2007-201681; National Institutes of Health grants R01DK093757, R01DK072193, U01DK105561, R01DK062370; National Human Genome Research Institute Division of Intramural Research project number Z01HG000024.

The authors of the **NEO study** thank all individuals who participated in the Netherlands Epidemiology in Obesity study, all participating general practitioners for inviting eligible participants and all research nurses for collection of the data. We thank the NEO study group, Pat van Beelen, Petra Noordijk and Ingeborg de Jonge for the coordination, lab and data management of the NEO study. The genotyping in the NEO study was supported by the Centre National de Génotypage (Paris, France), headed by Jean-Francois Deleuze. The NEO study is supported by the participating Departments, the Division and the Board of Directors of the Leiden University Medical Center, and by the Leiden University, Research Profile Area Vascular and Regenerative Medicine.

PIVUS/ULSAM studies were supported by Wellcome Trust Grants WT098017, WT064890, WT090532, Uppsala University, Uppsala University Hospital, the Swedish Research Council and the Swedish Heart-Lung Foundation.

The **RAINE study** was supported by the National Health and Medical Research Council of Australia [grant numbers 572613, 403981 and 003209] and the Canadian Institutes of Health Research [grant number MOP-82893]. The authors are grateful to the Raine Study participants and their families, and to the Raine Study research staff for cohort coordination and data collection. The authors gratefully acknowledge the NH&MRC for their long term contribution to funding the study over the last 29 years and also the following Institutions for providing funding for Core Management of the Raine Study: The University of Western Australia (UWA), Curtin University, Raine Medical Research Foundation, The Telethon Kids Institute, Women and Infants Research Foundation (King Edward Memorial Hospital), Murdoch University, The University of Notre Dame (Australia), and Edith Cowan University. The authors gratefully acknowledge the assistance of the Western Australian DNA Bank (National Health and Medical Research Council of Australia National Enabling Facility). This work was supported by resources provided by the Pawsey Supercomputing Centre with funding from the Australian Government and the Government of Western Australia.

The **RISC study** was supported by European Union grant QLG1-CT-2001-01252 and AstraZeneca. The initial genotyping of the RISC samples was funded by Merck & Co Inc.

RSI - The generation and management of the Illumina exome chip v1.0 array data for the Rotterdam Study (RS-I) was executed by the Human Genotyping Facility of the Genetic Laboratory of the Department of Internal Medicine, Erasmus MC, Rotterdam, The Netherlands. The Exome chip array data set was funded by the Genetic Laboratory of the Department of Internal Medicine, Erasmus MC, from

the Netherlands Genomics Initiative (NGI)/Netherlands Organisation for Scientific Research (NWO)-sponsored Netherlands Consortium for Healthy Aging (NCHA; project nr. 050-060-810); the Netherlands Organization for Scientific Research (NWO; project number 184021007) and by the Rainbow Project (RP10; Netherlands Exome Chip Project) of the Biobanking and Biomolecular Research Infrastructure Netherlands (BBMRI-NL; www.bbmri.nl). We thank Ms. Mila Jhamai, Ms. Sarah Higgins, and Mr. Marijn Verkerk for their help in creating the exome chip database, and Carolina Medina-Gomez, PhD , Lennard Karsten, MSc, and Linda Broer PhD for QC and variant calling. Variants were called using the best practice protocol developed by Grove et al. as part of the CHARGE consortium exome chip central calling effort. The Rotterdam Study is funded by Erasmus Medical Center and Erasmus University, Rotterdam, Netherlands Organization for the Health Research and Development (ZonMw), the Research Institute for Diseases in the Elderly (RIDE), the Ministry of Education, Culture and Science, the Ministry for Health, Welfare and Sports, the European Commission (DG XII), and the Municipality of Rotterdam. The authors are grateful to the study participants, the staff from the Rotterdam Study and the participating general practitioners and pharmacists. Additionally, the Netherlands Organization for Health Research and Development supported authors of this manuscript (C.M-G : ZonMw VIDI 016.136.367;).

Sorbs was supported by the Integrated Research and Treatment Center (IFB) Adiposity Diseases (K403, K737, AD2-7123). IFB is supported by the Federal Ministry of Education and Research (BMBF), Germany FKZ: 01EO1501. Sorbs was further supported by the German Research Foundation (CRC 1052 "Obesity mechanisms", A01; SPP 1629 TO 718/2-1) and by the German Diabetes Association.

TwinsUK is funded by the Wellcome Trust, Medical Research Council, European Union, the National Institute for Health Research (NIHR)-funded BioResource, Clinical Research Facility and Biomedical Research Centre based at Guy's and St Thomas' NHS Foundation Trust in partnership with King's College London.

The **WGHS** is supported by the National Heart, Lung, and Blood Institute (HL043851, HL080467, HL099355) and the National Cancer Institute (CA047988 and UM1CA182913) with collaborative scientific support and funding for genotyping provided by Amgen. Funding for leptin and adiponectin measures was provided by Roche.

The **Women's Health Initiative (WHI)** program is funded by the National Heart, Lung, and Blood Institute, National Institutes of Health, and the United States Department of Health and Human Services. Exome-chip data and analysis were supported through the Women's Health Initiative Sequencing Project (NHLBI RC2 HL-102924), the Genetics and Epidemiology of Colorectal Cancer Consortium (NCI CA137088), the Genomics and Randomized Trials Network (NHGRI U01-HG005152), and an NCI training grant (R25CA094880).

The **Young Finns Study** has been financially supported by the Academy of Finland: grants 286284, 134309 (Eye), 126925, 121584, 124282, 129378 (Salve), 117787 (Gendi), and 41071 (Skidi); the Social Insurance Institution of Finland; Competitive State Research Financing of the Expert Responsibility area of Kuopio, Tampere and Turku University Hospitals (grant X51001); Juho Vainio Foundation; Paavo Nurmi Foundation; Finnish Foundation for Cardiovascular Research ; Finnish Cultural Foundation; The Sigrid Juselius Foundation; Tampere Tuberculosis Foundation; Emil Aaltonen Foundation; Yrjö Jahnsson Foundation; Signe and Ane Gyllenberg Foundation; Diabetes Research Foundation of Finnish Diabetes Association; and EU Horizon 2020 (grant 755320 for TAXINOMISIS); and European Research Council (grant 742927 for MULTIEPIGEN project); Tampere University Hospital Supporting Foundation. We thank the teams that collected data at all measurement time points; the persons who participated as both

children and adults in these longitudinal studies; and biostatisticians Irina Lisinen, Johanna Ikonen, Noora Kartiosuo, Ville Aalto, and Jarno Kankaanranta for data management and statistical advice.

References

1. Andrieu, G., Quaranta, M., Leprince, C., and Hatzoglou, A. (2012). The GTPase Gem and its partner Kif9 are required for chromosome alignment, spindle length control, and mitotic progression. FASEB journal : official publication of the Federation of American Societies for Experimental Biology 26, 5025-5034.
2. Tikhonenko, I., Magidson, V., Graf, R., Khodjakov, A., and Koonce, M.P. (2013). A kinesin-mediated mechanism that couples centrosomes to nuclei. Cellular and molecular life sciences : CMLS 70, 1285-1296.
3. Fan, Y., Hanai, J.I., Le, P.T., Bi, R., Maridas, D., DeMambro, V., Figueroa, C.A., Kir, S., Zhou, X., Mannstadt, M., et al. (2017). Parathyroid Hormone Directs Bone Marrow Mesenchymal Cell Fate. Cell metabolism 25, 661-672.
4. Cawthorn, W.P., Scheller, E.L., Learman, B.S., Parlee, S.D., Simon, B.R., Mori, H., Ning, X., Bree, A.J., Schell, B., Broome, D.T., et al. (2014). Bone marrow adipose tissue is an endocrine organ that contributes to increased circulating adiponectin during caloric restriction. Cell metabolism 20, 368-375.
5. Tennenbaum, D.M., Manley, B.J., Zabor, E., Becerra, M.F., Carlo, M.I., Casuscelli, J., Redzematovic, A., Khan, N., Arcila, M.E., Voss, M.H., et al. (2017). Genomic alterations as predictors of survival among patients within a combined cohort with clear cell renal cell carcinoma undergoing cytoreductive nephrectomy. Urologic oncology 35, 532.e537-532.e513.
6. Chen, Z., Raghoonundun, C., Chen, W., Zhang, Y., Tang, W., Fan, X., and Shi, X. (2018). SETD2 indicates favourable prognosis in gastric cancer and suppresses cancer cell proliferation, migration, and invasion. Biochemical and biophysical research communications 498, 579-585.
7. Yuan, H., Li, N., Fu, D., Ren, J., Hui, J., Peng, J., Liu, Y., Qiu, T., Jiang, M., Pan, Q., et al. (2017). Histone methyltransferase SETD2 modulates alternative splicing to inhibit intestinal tumorigenesis. The Journal of clinical investigation 127, 3375-3391.
8. Husedzinovic, A., Neumann, B., Reymann, J., Draeger-Meurer, S., Chari, A., Erfle, H., Fischer, U., and Gruss, O.J. (2015). The catalytically inactive tyrosine phosphatase HD-PTP/PTPN23 is a novel regulator of SMN complex localization. Molecular biology of the cell 26, 161-171.
9. Smigiel, R., Landsberg, G., Schilling, M., Rydzanicz, M., Pollak, A., Walczak, A., Stodolak, A., Stawinski, P., Mierzewska, H., Sasiadek, M.M., et al. (2018). Developmental epileptic encephalopathy with hypomyelination and brain atrophy associated with PTPN23 variants affecting the assembly of UsnRNPs. European journal of human genetics : EJHG 26, 1502-1511.
10. Fan, C., Dong, L., Zhu, N., Xiong, Y., Zhang, J., Wang, L., Shen, Y., Zhang, X., and Chen, M. (2012). Isolation of siRNA target by biotinylated siRNA reveals that human CCDC12 promotes early erythroid differentiation. Leukemia research 36, 779-783.
11. London, E., Nesterova, M., Sinaii, N., Szarek, E., Chanturiya, T., Mastroyannis, S.A., Gavrilova, O., and Stratakis, C.A. (2014). Differentially regulated protein kinase A (PKA) activity in adipose tissue and liver is associated with resistance to diet-induced obesity and glucose intolerance in mice that lack PKA regulatory subunit type IIalpha. Endocrinology 155, 3397-3408.
12. Applegarth, D.A., and Toone, J.R. (2001). Nonketotic hyperglycinemia (glycine encephalopathy): laboratory diagnosis. Molecular genetics and metabolism 74, 139-146.
13. Ververi, A., Splitt, M., Dean, J.C.S., and Brady, A.F. (2018). Phenotypic spectrum associated with de novo mutations in QRICH1 gene. Clinical genetics 93, 286-292.
14. Pierre, G., Macdonald, A., Gray, G., Hendriksz, C., Preece, M.A., and Chakrapani, A. (2007). Prospective treatment in carnitine-acylcarnitine translocase deficiency. Journal of inherited metabolic disease 30, 815.

15. Lim, K.H., Choi, J.H., Park, J.H., Cho, H.J., Park, J.J., Lee, E.J., Li, L., Choi, Y.K., and Baek, K.H. (2016). Ubiquitin specific protease 19 involved in transcriptional repression of retinoic acid receptor by stabilizing CORO2A. Oncotarget 7, 34759-34772.
16. Bedard, N., Jammoul, S., Moore, T., Wykes, L., Hallauer, P.L., Hastings, K.E., Stretch, C., Baracos, V., Chevalier, S., Plourde, M., et al. (2015). Inactivation of the ubiquitin-specific protease 19 deubiquitinating enzyme protects against muscle wasting. FASEB journal : official publication of the Federation of American Societies for Experimental Biology 29, 3889-3898.
17. Zheng, B., Ma, Y.C., Ostrom, R.S., Lavoie, C., Gill, G.N., Insel, P.A., Huang, X.Y., and Farquhar, M.G. (2001). RGS-PX1, a GAP for GalphaS and sorting nexin in vesicular trafficking. Science (New York, NY) 294, 1939-1942.
18. Mas, C., Norwood, S.J., Bugarcic, A., Kinna, G., Leneva, N., Kovtun, O., Ghai, R., Ona Yanez, L.E., Davis, J.L., Teasdale, R.D., et al. (2014). Structural basis for different phosphoinositide specificities of the PX domains of sorting nexins regulating G-protein signaling. The Journal of biological chemistry 289, 28554-28568.
19. Chatterjee, T.K., Idelman, G., Blanco, V., Blomkalns, A.L., Piegore, M.G., Jr., Weintraub, D.S., Kumar, S., Rajsheker, S., Manka, D., Rudich, S.M., et al. (2011). Histone deacetylase 9 is a negative regulator of adipogenic differentiation. The Journal of biological chemistry 286, 27836-27847.
20. Chatterjee, T.K., Basford, J.E., Knoll, E., Tong, W.S., Blanco, V., Blomkalns, A.L., Rudich, S., Lentsch, A.B., Hui, D.Y., and Weintraub, N.L. (2014). HDAC9 knockout mice are protected from adipose tissue dysfunction and systemic metabolic disease during high-fat feeding. Diabetes 63, 176-187.
21. Schwefel, D., Arasu, B.S., Marino, S.F., Lamprecht, B., Kochert, K., Rosenbaum, E., Eichhorst, J., Wiesner, B., Behlke, J., Rocks, O., et al. (2013). Structural insights into the mechanism of GTPase activation in the GIMAP family. Structure (London, England : 1993) 21, 550-559.
22. Astle, W.J., Elding, H., Jiang, T., Allen, D., Ruklisa, D., Mann, A.L., Mead, D., Bouman, H., Riveros-Mckay, F., Kostadima, M.A., et al. (2016). The Allelic Landscape of Human Blood Cell Trait Variation and Links to Common Complex Disease. Cell 167, 1415-1429.e1419.
23. Houchens, C.R., Montigny, W., Zeltser, L., Dailey, L., Gilbert, J.M., and Heintz, N.H. (2000). The dhfr oribeta-binding protein RIP60 contains 15 zinc fingers: DNA binding and looping by the central three fingers and an associated proline-rich region. Nucleic acids research 28, 570-581.
24. Ruschke, K., Illes, M., Kern, M., Kloting, I., Fasshauer, M., Schon, M.R., Kosacka, J., Fitzl, G., Kovacs, P., Stumvoll, M., et al. (2010). Repin1 maybe involved in the regulation of cell size and glucose transport in adipocytes. Biochemical and biophysical research communications 400, 246-251.
25. Kunath, A., Hesselbarth, N., Gericke, M., Kern, M., Dommel, S., Kovacs, P., Stumvoll, M., Bluher, M., and Kloting, N. (2016). Repin1 deficiency improves insulin sensitivity and glucose metabolism in db/db mice by reducing adipose tissue mass and inflammation. Biochemical and biophysical research communications 478, 398-402.
26. Helfer, G., and Wu, Q.F. (2018). Chemerin: a multifaceted adipokine involved in metabolic disorders. The Journal of endocrinology 238, R79-r94.
27. Goralski, K.B., McCarthy, T.C., Hanniman, E.A., Zabel, B.A., Butcher, E.C., Parlee, S.D., Muruganandan, S., and Sinal, C.J. (2007). Chemerin, a novel adipokine that regulates adipogenesis and adipocyte metabolism. The Journal of biological chemistry 282, 28175-28188.
28. Condamine, T., Le Texier, L., Howie, D., Lavault, A., Hill, M., Halary, F., Cobbold, S., Waldmann, H., Cuturi, M.C., and Chiffoleau, E. (2010). Tmem176B and Tmem176A are associated with the immature state of dendritic cells. Journal of leukocyte biology 88, 507-515.
29. Kirschner, K.M., Braun, J.F., Jacobi, C.L., Rudigier, L.J., Persson, A.B., and Scholz, H. (2014). Amine oxidase copper-containing 1 (AOC1) is a downstream target gene of the Wilms tumor protein, WT1, during kidney development. The Journal of biological chemistry 289, 24452-24462.

30. Sass, J.O., Gemperle-Britschgi, C., Tarailo-Graovac, M., Patel, N., Walter, M., Jordanova, A., Alfadhel, M., Baric, I., Coker, M., Damli-Huber, A., et al. (2016). Unravelling 5-oxoprolinuria (pyroglutamic aciduria) due to bi-allelic OPLAH mutations: 20 new mutations in 14 families. Molecular genetics and metabolism 119, 44-49.
31. Rideout, E.J., Marshall, L., and Grewal, S.S. (2012). Drosophila RNA polymerase III repressor Maf1 controls body size and developmental timing by modulating tRNAiMet synthesis and systemic insulin signaling. Proceedings of the National Academy of Sciences of the United States of America 109, 1139-1144.
32. Khanna, A., Johnson, D.L., and Curran, S.P. (2014). Physiological roles for mafr-1 in reproduction and lipid homeostasis. Cell reports 9, 2180-2191.
33. Willis, I.M. (2018). Maf1 phenotypes and cell physiology. Biochimica et biophysica acta Gene regulatory mechanisms 1861, 330-337.
34. Palian, B.M., Rohira, A.D., Johnson, S.A., He, L., Zheng, N., Dubeau, L., Stiles, B.L., and Johnson, D.L. (2014). Maf1 is a novel target of PTEN and PI3K signaling that negatively regulates oncogenesis and lipid metabolism. PLoS genetics 10, e1004789.
35. Khanna, A., Pradhan, A., and Curran, S.P. (2015). Emerging Roles for Maf1 beyond the Regulation of RNA Polymerase III Activity. Journal of molecular biology 427, 2577-2585.
36. Poulter, J.A., Al-Araimi, M., Conte, I., van Genderen, M.M., Sheridan, E., Carr, I.M., Parry, D.A., Shires, M., Carrella, S., Bradbury, J., et al. (2013). Recessive mutations in SLC38A8 cause foveal hypoplasia and optic nerve misrouting without albinism. American journal of human genetics 93, 1143-1150.
37. Yamauchi, T., Kamon, J., Ito, Y., Tsuchida, A., Yokomizo, T., Kita, S., Sugiyama, T., Miyagishi, M., Hara, K., Tsunoda, M., et al. (2003). Cloning of adiponectin receptors that mediate antidiabetic metabolic effects. Nature 423, 762-769.
38. Hug, C., Wang, J., Ahmad, N.S., Bogan, J.S., Tsao, T.S., and Lodish, H.F. (2004). T-cadherin is a receptor for hexameric and high-molecular-weight forms of Acrp30/adiponectin. Proceedings of the National Academy of Sciences of the United States of America 101, 10308-10313.
39. Sakai, J., Rawson, R.B., Espenshade, P.J., Cheng, D., Seegmiller, A.C., Goldstein, J.L., and Brown, M.S. (1998). Molecular identification of the sterol-regulated luminal protease that cleaves SREBPs and controls lipid composition of animal cells. Molecular cell 2, 505-514.
40. Ramos-Lopez, O., Riezu-Boj, J.I., Milagro, F.I., and Martinez, J.A. (2018). DNA methylation signatures at endoplasmic reticulum stress genes are associated with adiposity and insulin resistance. Molecular genetics and metabolism 123, 50-58.
41. Lundback, V., Kulyte, A., Strawbridge, R.J., Ryden, M., Arner, P., Marcus, C., and Dahlman, I. (2018). FAM13A and POM121C are candidate genes for fasting insulin: functional follow-up analysis of a genome-wide association study. Diabetologia 61, 1112-1123.
42. Wardhana, D.A., Ikeda, K., Barinda, A.J., Nugroho, D.B., Qurania, K.R., Yagi, K., Miyata, K., Oike, Y., Hirata, K.I., and Emoto, N. (2018). Family with sequence similarity 13, member A modulates adipocyte insulin signaling and preserves systemic metabolic homeostasis. Proceedings of the National Academy of Sciences of the United States of America 115, 1529-1534.
43. He, L., Girijashanker, K., Dalton, T.P., Reed, J., Li, H., Soleimani, M., and Nebert, D.W. (2006). ZIP8, member of the solute-carrier-39 (SLC39) metal-transporter family: characterization of transporter properties. Molecular pharmacology 70, 171-180.
44. Zhang, R., Witkowska, K., Afonso Guerra-Assuncao, J., Ren, M., Ng, F.L., Mauro, C., Tucker, A.T., Caulfield, M.J., and Ye, S. (2016). A blood pressure-associated variant of the SLC39A8 gene influences cellular cadmium accumulation and toxicity. Human molecular genetics 25, 4117-4126.

45. Lin, W., Vann, D.R., Doulias, P.T., Wang, T., Landesberg, G., Li, X., Ricciotti, E., Scalia, R., He, M., Hand, N.J., et al. (2017). Hepatic metal ion transporter ZIP8 regulates manganese homeostasis and manganese-dependent enzyme activity. The Journal of clinical investigation 127, 2407-2417.
46. Boycott, K.M., Beaulieu, C.L., Kernohan, K.D., Gebril, O.H., Mhanni, A., Chudley, A.E., Redl, D., Qin, W., Hampson, S., Kury, S., et al. (2015). Autosomal-Recessive Intellectual Disability with Cerebellar Atrophy Syndrome Caused by Mutation of the Manganese and Zinc Transporter Gene SLC39A8. American journal of human genetics 97, 886-893.
47. Pickrell, J.K., Berisa, T., Liu, J.Z., Segurel, L., Tung, J.Y., and Hinds, D.A. (2016). Detection and interpretation of shared genetic influences on 42 human traits. Nature genetics 48, 709-717.
48. Nagai, Y., Nishimura, A., Tago, K., Mizuno, N., and Itoh, H. (2010). Ric-8B stabilizes the alpha subunit of stimulatory G protein by inhibiting its ubiquitination. The Journal of biological chemistry 285, 11114-11120.
49. Maureira, A., Sanchez, R., Valenzuela, N., Torrejon, M., Hinrichs, M.V., Olate, J., and Gutierrez, J.L. (2016). The CREB Transcription Factor Controls Transcriptional Activity of the Human RIC8B Gene. Journal of cellular biochemistry 117, 1797-1805.
50. Griebel, G., Ravinet-Trillou, C., Beeske, S., Avenet, P., and Pichat, P. (2014). Mice deficient in cryptochrome 1 (cry1 (-/-)) exhibit resistance to obesity induced by a high-fat diet. Frontiers in endocrinology 5, 49.
51. Jang, H., Lee, G.Y., Selby, C.P., Lee, G., Jeon, Y.G., Lee, J.H., Cheng, K.K., Titchenell, P., Birnbaum, M.J., Xu, A., et al. (2016). SREBP1c-CRY1 signalling represses hepatic glucose production by promoting FOXO1 degradation during refeeding. Nat Commun 7, 12180.
52. Calabrese, G.M., Mesner, L.D., Stains, J.P., Tommasini, S.M., Horowitz, M.C., Rosen, C.J., and Farber, C.R. (2017). Integrating GWAS and Co-expression Network Data Identifies Bone Mineral Density Genes SPTBN1 and MARK3 and an Osteoblast Functional Module. Cell systems 4, 46-59.e44.
53. Hyvarinen, A.K., Pohjoismaki, J.L., Holt, I.J., and Jacobs, H.T. (2011). Overexpression of MTERFD1 or MTERFD3 impairs the completion of mitochondrial DNA replication. Molecular biology reports 38, 1321-1328.
54. Manenschijn, L., van den Akker, E.L., Lamberts, S.W., and van Rossum, E.F. (2009). Clinical features associated with glucocorticoid receptor polymorphisms. An overview. Annals of the New York Academy of Sciences 1179, 179-198.
55. Peckett, A.J., Wright, D.C., and Riddell, M.C. (2011). The effects of glucocorticoids on adipose tissue lipid metabolism. Metabolism: clinical and experimental 60, 1500-1510.
56. Ferrau, F., and Korbonits, M. (2015). Metabolic comorbidities in Cushing's syndrome. European journal of endocrinology / European Federation of Endocrine Societies 173, M133-157.
57. Lee, M.J., and Fried, S.K. (2014). The glucocorticoid receptor, not the mineralocorticoid receptor, plays the dominant role in adipogenesis and adipokine production in human adipocytes. International journal of obesity (2005) 38, 1228-1233.
58. Pantoja, C., Huff, J.T., and Yamamoto, K.R. (2008). Glucocorticoid signaling defines a novel commitment state during adipogenesis in vitro. Molecular biology of the cell 19, 4032-4041.
59. Shen, Y., Roh, H.C., Kumari, M., and Rosen, E.D. (2017). Adipocyte glucocorticoid receptor is important in lipolysis and insulin resistance due to exogenous steroids, but not insulin resistance caused by high fat feeding. Molecular metabolism 6, 1150-1160.
60. Estep, P.W., 3rd, Warner, J.B., and Bulyk, M.L. (2009). Short-term calorie restriction in male mice feminizes gene expression and alters key regulators of conserved aging regulatory pathways. PloS one 4, e5242.
61. Chu, A.Y., Deng, X., Fisher, V.A., Drong, A., Zhang, Y., Feitosa, M.F., Liu, C.T., Weeks, O., Choh, A.C., Duan, Q., et al. (2017). Multiethnic genome-wide meta-analysis of ectopic fat depots identifies loci associated with adipocyte development and differentiation. Nature genetics 49, 125-130.